BNL-221015-2021-TECH
C-A/AP/639

FY2020-21 parameters for Gold ions in Booster, AGS, and RHIC

C. Gardner

February 2021

Collider Accelerator Department
Brookhaven National Laboratory

U.S. Department of Energy
USDOE Office of Science (SC), Nuclear Physics (NP) (SC-26)

DISCLAIMER

FY2020–21 parameters for Gold ions in Booster, AGS, and RHIC

C.J. Gardner

February 7, 2021

Sections **1** through **6** of this report give parameters for **low-energy** gold ions circulating in RHIC at injection and in AGS at extraction.

Section **7** gives parameters for Au79+ ions circulating in RHIC at the standard injection magnetic rigidity of 81.11378003 Tm.

Sections **8** through **10** give parameters for **medium-energy** Au79+ ions circulating in RHIC at 31.2, 26.5, 19.5, 13.5 GeV per nucleon. To reach these energies, acceleration in RHIC is required. The magnetic rigidity at RHIC injection for these setups is 60.3050632557 Tm. The corresponding ion energy is 7.30950517185 GeV per nucleon.

The parameters for the **standard setup** of gold ions in Booster, AGS, and RHIC are documented in [1, 2]. For convenience they are listed here in Sections **11** through **13**. The standard setup uses gold ions from EBIS.

For operation of RHIC with Au79+ ions at 3.846682 and 5.761022 GeV per nucleon, gold ions are provided by **Tandem**. Some of the parameters specific to this setup are given in Sections **14** and **15**. In order to achieve a single bunch of Tandem ions at Booster extraction, a 6 to 3 to 1 bunch merge is required. This has been developed by Keith Zeno and is documented in [3, 4, 5, 6, 7].

Different **bunch merges and fill patterns** in AGS are used depending on the desired bunch intensity, longitudinal emittance, and number of bunches to be injected into RHIC per AGS cycle. These are described in Sections **16** through **27**. The bunch merges of the standard setup are documented in [1, 2].

Bucket and bunch parameters for clean injection of low-energy gold ions into RHIC are documented in [8]. Parameters of **past medium and low energy** gold ion setups are documented in [9].

Sections 28 through **36** give calculations of heating and cooling in the BTA stripping foils and the AGS beam dump and plunging stripping foil.

1 Electron RF frequency

The Au79+ ions circulating in RHIC at low energy are cooled with a beam of bunched electrons. The RF frequency f_E used for acceleration of the bunches needs to be synchronized with the revolution frequency f of the gold ions in the collider. This is accomplished by imposing the constraint [10]

$$nf = f_E \tag{1}$$

where

$$f_E = 704.005148 \text{ MHz} \tag{2}$$

and n is a positive integer.

The parameters listed in **Sections 3** through **6** are obtained by taking

$$n = 9279,\ 9194,\ 9123,\ 9077,\ 9044 \tag{3}$$

for energies 1, 2, 3, 4, 5, respectively. These numbers are the same as those used in 2019.

2 Gold ion mass

The values of the fundamental constants listed on page one of C-A/AP/Note 574 [2] give

$$mc^2 = 183.433\,337\,044 \text{ GeV} \tag{4}$$

for the mass-energy equivalent of the Au79+ ion.

More recent values of the fundamental constants, listed on page eleven of C-A/AP/Note 608 [11], give

$$mc^2 = 183.433\,343\,902 \text{ GeV}. \tag{5}$$

The fractional difference between these two values amounts to

$$\frac{183.433\,343\,902 - 183.433\,337\,044}{183.433\,337\,044} = 3.74 \times 10^{-8} \tag{6}$$

which, for the computation of various parameters that appear in this note, is entirely negligible. (These details are included because of recent controversy about the mass of the ion.)

3 RHIC injection energies 1, 2, 3

	Energy 1	Energy 2	Energy 3	Unit
Q	79	79	79	
mc^2	183.433343902	183.433343902	183.433343902	GeV
W/A	2.91554792413	3.66145111778	4.82988847577	GeV
cp/A	3.73228478257	4.49720196646	5.68527631587	GeV
E/A	**3.84668164952**	**4.59258484317**	**5.76102220117**	GeV
$B\rho$	31.0451102170	37.4076842606	47.2900756836	Tm
β	0.970260895656	0.979231112769	0.986852006006	
γ	4.13118067214	4.93225056501	6.18710507853	
η	-0.05669	-0.03920	-0.02421	
n	**9279**	**9194**	**9123**	
f	75.8707994396	76.5722371112	77.1681626658	KHz
h	123	122	121	
hf	9.33210833107	9.34181292756	9.33734768256	MHz
$3hf$	27.99632499321	28.02543878268	28.01204304768	MHz
δC	0	0	0	mm

4 Corresponding AGS extraction parameters

	Energy 1	Energy 2	Energy 3	Unit
Q	77	77	77	
mc^2	183.434181300	183.434181300	183.434181300	GeV
W/A	2.91556123404	3.66146783289	4.82991052486	GeV
cp/A	3.73230182100	4.49722249689	5.68530226992	GeV
E/A	**3.84669921018**	**4.59260580903**	**5.76104850101**	GeV
$B\rho$	31.8516221228	38.3794876307	48.5186108306	Tm
β	0.970260895657	0.979231112770	0.986852006006	
γ	4.13118067219	4.93225056511	6.18710507853	
η	-0.04475	-0.02727	-0.01228	
h	12	12	12	
hf	4.32463556806	4.36461751534	4.39858527195	MHz
T/h	231.233356953	229.115150752	227.345825572	ns
R	128.457981391	128.457981391	128.457981391	m

5 RHIC injection energies 4, 5

	Energy 4	Energy 5	Unit
Q	79	79	
mc^2	183.433343902	183.433343902	GeV
W/A	6.37837144646	8.86482729097	GeV
cp/A	7.24995557522	9.75160716085	GeV
E/A	**7.30950517185**	**9.79596101636**	GeV
$B\rho$	60.3050632557	81.1137779506	Tm
β	0.991853128875	0.995472230296	
γ	7.85011322489	10.5204663404	
η	-0.01432	-0.007126	
n	**9077**	**9044**	
f	77.5592319048	77.8422321981	KHz
h	120	120	
hf	9.30710782858	9.34106786378	MHz
$3hf$	27.92132348573	28.02320359133	MHz
δC	0	0	mm

6 Corresponding AGS extraction parameters

	Energy 4	Energy 5	Unit
Q	77	77	
mc^2	183.434181300	183.434181300	GeV
W/A	6.37840056414	8.86486775910	GeV
cp/A	7.24998867180	9.75165167725	GeV
E/A	**7.30953854028**	**9.79600573525**	GeV
$B\rho$	61.8717109827	83.2210092307	Tm
β	0.991853128874	0.995472230295	
γ	7.85011322442	10.5204663393	
η	-0.002387	0.004806	
h	12	12	
hf	4.42087621857	4.43700723529	MHz
T/h	226.199502216	225.377139809	ns
R	128.457981391	128.457981391	m

7 Standard RHIC injection [2] versus energy 5

	Standard	Energy 5	Unit
Q	79	79	
mc^2	183.433343902	183.433343902	GeV
W/A	8.86482753983	8.86482729097	GeV
cp/A	9.75160741084	9.75160716085	GeV
E/A	9.79596126523	9.79596101636	GeV
$B\rho$	**81.1137800300**	**81.1137779506**	Tm
β	0.995472230526	0.995472230296	
γ	10.5204666076	10.5204663404	
η	-0.007126	-0.007126	
n	N/A	**9044**	
f	77.8422322162	77.8422321981	KHz
h	360	120	
hf	28.0232035978	9.34106786378	MHz
δC	0	0	mm

8 Gold in RHIC at 31.2 GeV per nucleon

Parameter	Injection	Transition	Store	Unit
Q	79	79	79	
mc^2	183.433343902	183.433343902	183.433343902	GeV
W/A	6.37837144646	20.3825172488	30.2688662746	GeV
cp/A	7.24995557522	21.2933019477	31.1861025135	GeV
E/A	**7.30950517185**	21.3136509742	**31.2**	GeV
$B\rho$	60.3050632557	177.117488177	259.405711561	Tm
β	0.991853128875	0.999045258528	0.999554567742	
γ	7.85011322489	**22.8900**	33.5075394105	
η	-0.01432	0.0	0.00102	
f	77.5592319048	78.1216297391	78.1614558286	kHz
h	360	360	360	
hf	27.92132348573	28.1237867061	28.1381240983	MHz
δC	0	0	0	mm

9 Gold in RHIC at 26.5 & 19.5 GeV per nucleon

Parameter	Injection	Store	Store	Unit
Q	79	79	79	
mc^2	183.433343902	183.433343902	183.433343902	GeV
W/A	6.37837144646	25.5688662746	18.5688662746	GeV
cp/A	7.24995557522	26.4836362682	19.4777562872	GeV
E/A	**7.30950517185**	**26.5**	**19.5**	GeV
$B\rho$	60.3050632557	220.290640932	162.015796207	Tm
β	0.991853128875	0.999382500686	0.998859296782	
γ	7.85011322489	28.4599293070	20.9422121315	
η	-0.01432	0.000674	-0.0003715	
f	77.5592319048	78.1480008237	78.1070882211	kHz
h	360	360	360	
hf	27.92132348573	28.13328029655	28.1185517596	MHz
δC	0	0	0	mm

10 Gold in RHIC at 13.5 GeV per nucleon

Parameter	Injection	Transition	Store	Unit
Q	79	79	79	
mc^2	183.433343902	183.433343902	183.433343902	GeV
W/A	6.37837144646	20.3825172488	12.5688662746	GeV
cp/A	7.24995557522	21.2933019477	13.4678502362	GeV
E/A	**7.30950517185**	21.3136509742	**13.5**	GeV
$B\rho$	60.3050632557	177.117488177	112.025453396	Tm
β	0.991853128875	0.999045258528	0.997618536017	
γ	7.85011322489	**22.8900**	14.4984545526	
η	-0.01432	0.0	-0.00285	
f	77.5592319048	78.1216297391	78.0100653362	kHz
h	360	360	360	
hf	27.92132348573	28.1237867061	28.08362352105	MHz
δC	0	0	0	mm

11 Gold in Booster (standard setup) [2]

Parameter	Injection	Merge porch	Extraction	Unit
Q	32	32	32	
mc^2	183.456851494	183.456851494	183.456851494	GeV
W/A	1.9762739452	72.089750	107.75879	MeV
cp/A	60.701960016	373.44950	460.77475	MeV
E/A	0.9332293272	1.0033428	1.0390118	GeV
$B\rho$	1.24651715338	7.6688003	9.46202773202	Tm
β	0.065045062608	0.37220529	0.44347401	
$\gamma - 1$	0.002122166406	0.07741156	0.11571376	
η	-0.953	-0.8186	-0.7605	
ϵ_H (95%)	12.1π	12.1π	12.1π	mm mrad
ϵ_V (95%)	5.68π	5.68π	5.68π	mm mrad
h	4	1	1	
hf	**386.560**	**553.000**	**658.910**	KHz
R	$201.780/(2\pi)$	$201.780/(2\pi)$	128.4526/4	m

Here ϵ_H and ϵ_V are the normalized horizontal and vertical transverse emittances. These follow from the assumption that during injection the horizontal and vertical acceptances in Booster are completely filled. The horizontal and vertical acceptances are 185π and 87π mm mrad (un-normalized) respectively.

Parm	Injection	Ext	Ext	Ext	Unit
V_g	5.730	25.2	25.2	25.2	kV
A_S	16.076	318.54	318.54	318.54	eV s
dB/dt	0	**70**	**35**	**0**	G/ms
ϕ_s	0	50.999	22.866	0	deg
F_s	1.1557	0.8139	0.9849	1.0260	kHz
$A_{\rm bk}$	16.076	36.294	140.88	318.54	eV s
A_b	1.82	13.987	13.987	13.987	eV s
Δt	635.1	264.6	235.1	229.8	ns
ΔE	1.836	34.11	38.00	38.84	MeV

Parameter	Injection	Extraction	Unit
No. Bunches	4	1	
Bucket Width	2586.92053	1517.65795	ns
Ions/Bunch	1.25/4	1.04	10^9
Bunch Area	0.037/4	0.071	eV s/A

12 Gold in AGS (standard setup) [2]

Parameter	Injection	Porch	Extraction	Unit
Q	77	77	77	
mc^2	183.434174442	183.434174442	183.434174442	GeV
W/A	0.10529199	0.16448553	8.86486804031	GeV
cp/A	0.45515837	0.57738456	9.75165192809	GeV
E/A	1.0364299	1.09562347	9.79600598164	GeV
$B\rho$	3.88434088	4.9274243	83.2210113714	Tm
β	0.43915981	0.52699177	0.995472230863	
γ	1.1130788	1.1766500	10.5204669972	
η	-0.793	-0.708	0.00481	
$\beta\gamma$	0.48881949	0.62008488	10.472833	
$\beta\gamma^2$	0.54409463	0.72962288	110.17909	
h	24	4	12	
hf	**3.915000**	**0.783**	**4.43700723782**	MHz
R	128.4526	128.4526	128.457981391	m

Parameter	Inj	Porch	Porch	Ext	Unit
h	24	12	4	12	
V_g	119.8	100	15.0	185.2	kV
A_S	35.84	100.8	202.8	4979	eV s
dB/dt	0	0	0	0	G/ms
ϕ_s	0	0	0	180	degrees
F_s	4.346	2.581	0.577	0.0967	kHz
$A_{\rm bk}$	35.84	100.8	202.8	4979	eV s
A_b	17.73	39.4	118.2	147.75	eV s
Δt	140	203	775	28.0	ns
ΔE	83.6	127	102	3365	MeV

Parameter	Inj	Porch	Porch	Ext	Unit
h	24	12	4	12	
Bucket Width	255.428	425.713	1277.139	225.377	ns
No. of Bunches	12	6	2	2	
Ions/Bunch	0.53	1.06	3.18	3.0	10^9
Bunch Area	0.09	0.20	0.60	0.75	eV s/A

13 Gold in RHIC (standard setup) [2]

Parameter	Injection	Transition	Store	Unit
Q	79	79	79	
mc^2	183.433337044	183.433337044	183.433337044	GeV
W/A	8.86482757134	20.3825164868	99.0688663094	GeV
cp/A	9.75160741084	21.2933011516	99.9956648563	GeV
E/A	9.79596126192	21.3136501774	**100.000**	GeV
$B\rho$	**81.11378003**	177.117481555	831.763013151	Tm
β	0.995472230863	0.999045258528	0.999956648563	
γ	10.5204669974	**22.8900**	107.395963664	
η	-0.00713	0.0	0.00182	
f	77.8422322425	78.1216297391	78.1928970559	kHz
h	360	360	2520	
hf	28.0232036073	28.1237867061	197.046100581	MHz
δC	0	0	0	mm

Parameter	Injection	Store	Unit
h	360	2520	
V_g	393.1	3000	kV
A_S	174.4	164.4	eV s
dB/dt	0	0	G/ms
ϕ_s	0	180	degrees
F_s	0.200	0.232	kHz
A_{bk}	174.4	164.4	eV s
A_b	137.9	137.9	eV s
A_b	0.70	0.70	eV s/A
Δt	26.8	4.00	ns
ΔE	3549	24052	MeV

14 Tandem Au31+ in Booster

At injection as documented in C-A/AP/Note 397 [12]:

1. $B\rho = 0.8813444$ Tm
2. $B = 635.633798754$ Gauss
   (629.5 Gauss measured)
3. Inflector $V = 28.312$ KV
4. $f = 66.2678758864$ kHz
5. $6f = 397.607255319$ kHz
6. $W/A = 0.927701900621$ MeV per nucleon

Note that the inflector voltage given above is higher than that given in [12]. This is because the distance between the cathode and septum of the inflector was increased from 17 to 21 mm prior to RHIC Run 12.

On the 6 to 3 to 1 merge porch as documented in [6]:

1. $f = 396.830$ kHz
2. $6f = 2.38098$ MHz
3. $B\rho = 5.47124229551$ Tm
4. $B = 3.94591095626$ kG
5. $W/A = 35.1071306278$ MeV per nucleon

At extraction with same $B\rho$ as setup for Au32+ ions from EBIS:

1. $B\rho = 9.46202773202$ Tm
2. $B = 6.82973330029$ kG
3. $f = 642.214748437$ kHz
4. $W/A = 101.453506352$ MeV per nucleon

After extraction, the Au31+ ions pass through two stripping foils in the BTA line. The resulting Au77+ ions are then selected for injection into AGS. The revolution frequency of the ions circulating in AGS at injection is calculated in the next section.

15 Energy loss in BTA stripper for setup that uses Au31+ ions provided by Tandem

The stripper used to strip gold ions in the BTA transfer line consists of a 6.45 mg/cm^2 aluminum foil followed by a 8.39 mg/cm^2 "glassy" carbon foil [13, 14]. We can estimate the energy loss in the foils as follows:

The kinetic energy of a proton that has the same velocity as the Au31+ ion just upstream of the aluminum foil is

$$W_p = 102.2 \text{ MeV}. \tag{7}$$

The rate of energy loss of a proton passing through the foil with kinetic energy W_p is [15]

$$-\frac{dE_p}{dx} = 5.589 \text{ MeV cm}^2/\text{g}. \tag{8}$$

The rate of energy loss of the Au77+ ion is obtained by scaling the Bethe-Bloch result for protons [16]. Thus

$$-\frac{dE}{dx} = -Q^2 \frac{dE_p}{dx} \tag{9}$$

where $Q = 77$. Multiplying this by the surface density of the aluminum foil (6.45 mg/cm^2) gives

$$\Delta E_a = 1.085 \text{ MeV per nucleon}. \tag{10}$$

This is the energy lost by the Au77+ ion upon passing through the aluminum foil. The kinetic energy of a proton that has the same velocity as the Au77+ ion just downstream of the aluminum foil is then

$$W_p = 101.1 \text{ MeV}. \tag{11}$$

The rate of energy loss of a proton passing through the carbon foil with this kinetic energy is [15]

$$-\frac{dE_p}{dx} = 6.468 \text{ MeV cm}^2/\text{g}. \tag{12}$$

Using this result in (9) with $Q = 77$, and multiplying by the surface density of the carbon foil (8.39 mg/cm^2) gives

$$\Delta E_c = 1.633 \text{ MeV per nucleon}. \tag{13}$$

The total energy lost upon passing through both foils is then

$$\Delta E = \Delta E_a + \Delta E_c = 2.718 \text{ MeV per nucleon.} \tag{14}$$

This gives revolution frequency

$$f = \underline{158.696 \text{ kHz}} \tag{15}$$

for the Au77+ ions circulating in AGS at injection. The corresponding magnetic rigidity is

$$B\rho = 3.75492421176 \text{ Tm.} \tag{16}$$

16 The 5.75 GeV per nucleon Setup

This energy is actually Energy 3 listed in **Sections 3** and **4**. It is called 5.75 for convenience. The setup, developed by K. Zeno [5, 7], uses Au31+ ions from Tandem with 8 single-bunch transfers from Booster to AGS per AGS cycle. The AGS fill pattern and 2 to 1 merge used are described in **Section 26**. These give 4 bunches at AGS extraction, each of which contains, in effect, two Booster loads. The use of Tandem beam here is a departure from the standard setup which uses Au32+ ions from EBIS. This was done in order to have bunches with sufficiently low longitudinal emittance and sufficiently high intensity at AGS extraction.

Because Tandem is capable of delivering significantly more beam per pulse than EBIS [17], and because we now have more transfers from Booster to AGS (per AGS cycle), it is easy with Tandem to exceed the maximum beam intensity previously achieved in AGS. That maximum was 7.4e9 Au77+ ions circulating in AGS at 9.8 GeV per nucleon as reported in [7]. Going to the higher intensities needed for the 5.75 setup required a review to ensure that measures were in place to prevent damage to the beam dump and the plunging stripping foil (PSF). These components, along with the closed orbit bump at the dump, ensure that any beam not extracted from AGS is put into the water-cooled copper absorber of the dump [18]. This is absolutely essential because the highly charged Au77+ ions can cause significant damage if lost on the vacuum chamber wall. (The amount of energy deposited is proportional to the square of the ion charge.) The review, followed by observations of the effect of higher intensities on the PSF, showed that with certain precautions and procedures it is reasonable to increase the maximum intensity to 9.6e9 Au77+ ions per AGS cycle at 5.75 GeV per nucleon. Those precautions

and accompanying procedures are given in [19]. As of this writing, a new document [20] allows the same maximum intensity for Au77+ ions at 3.85 GeV per nucleon. For all other gold ion energies, the maximum intensity currently allowed is 8e9 Au77+ ions circulating in AGS at extraction.

Another component affected by the intensity of gold beam is the BTA stripper. The stripping foils used here are the aluminum-carbon foils described in the previous section. In order to get a given number of Au77+ ions circulating in AGS at extraction, one needs approximately twice as many ions passing through the foils. For the past decade the foils have given no indication of degradation when exposed to intensities of 12.0e9 gold ions per AGS cycle or less. However, when exposed to intensities ranging from 16.0e9 to 20.0e9 gold ions per AGS cycle, the foils accumulate damage and their performance suffers significantly. This has been quantified by careful measurements of stripping efficiency carried out by K. Zeno and documented in [7]. It is found that any area on a foil that is exposed to the higher intensities can have a useful lifetime of just hours. By moving the position of the beam on the foil or by moving the position of the foil itself, one can make use of any available undamaged area. Eventually all the undamaged area is used up and the foil is spent. Calculations of the heating and radiative cooling of the aluminum and carbon foils are carried out in **Sections 28** through **30**. These show that with 20.0e9 gold ions incident on the foils (per AGS cycle), the aluminum comes very close to its melting point. The carbon, on the other hand, does not melt and stays well below its sublimation temperature.

In November 2020, the aluminum-carbon foils that had been in place since 2010 were removed from the foil changer and replaced with three new aluminum-carbon foils. These now occupy slots 5, 6, and 7 in the changer. (There are 8 slots which are labeled 0 through 7. Slot 0 is empty. Slots 1 and 2 contain nickel-aluminum foils that are used to strip uranium ions. Slots 3 and 4 contain new aluminum foils that will be used to strip oxygen ions.) Pictures of the old aluminum-carbon foils removed from slots 5 and 6 are shown in [7]. There one sees the significant damage done to the aluminum foils by the high-intensity beam. In order to conserve the new foils, they should be exposed to high-intensity beam only when high intensity is needed. This is normally during RHIC fills or when preparing for a fill. The transfer efficiency between Booster and AGS should be monitored to ensure that it is nominal. If lower than nominal, more beam is being put into the foil than necessary to produce a given intensity in AGS. This unnecessarily reduces the lifetime of the foils.

17 The 4.59 GeV per nucleon Setups

This energy is actually Energy 2 listed in **Sections 3** and **4**. It is called 4.59 for convenience. Three setups, A, B, and C, have been used at this energy. All three use Au32+ ions from EBIS.

Setup A uses 12 single-bunch transfers from Booster to AGS per AGS cycle. The AGS fill pattern and 3 to 1 merge used are described in **Section 24**. These give 4 bunches at AGS extraction, each of which contains, in effect, three Booster loads.

Setup B also uses 12 single-bunch transfers from Booster to AGS per AGS cycle, but a 4 to 1 merge is used instead of a 3 to 1. The AGS fill pattern and merge are described in **Section 23**. These give 3 bunches at AGS extraction, each of which contains, in effect, four Booster loads.

Setup C uses 9 single-bunch transfers from Booster to AGS per AGS cycle. The AGS fill pattern and alternate 3 to 1 merge used are described in **Section 25**. These give 3 bunches at AGS extraction, each of which contains, in effect, three Booster loads.

A setup that uses Au31+ ions from Tandem was also used. This was developed by K. Zeno and is documented in [7].

18 The 7.3 GeV per nucleon Setup

This energy is actually Energy 4 listed in **Sections 5** and **6**. It is called 7.3 for convenience. The setup uses Au32+ ions from EBIS with 12 single-bunch transfers from Booster to AGS per AGS cycle. The AGS fill pattern and 6 to 1 merge used are described in **Section 22**. These give 2 bunches at AGS extraction, each of which contains, in effect, six Booster loads.

19 The 3.85 GeV per nucleon Setup

This energy is actually Energy 1 listed in **Sections 3** and **4**. It is called 3.85 for convenience. The setup is essentially the same as the 5.75 GeV setup. It is documented in [7].

20 AGS injection timing

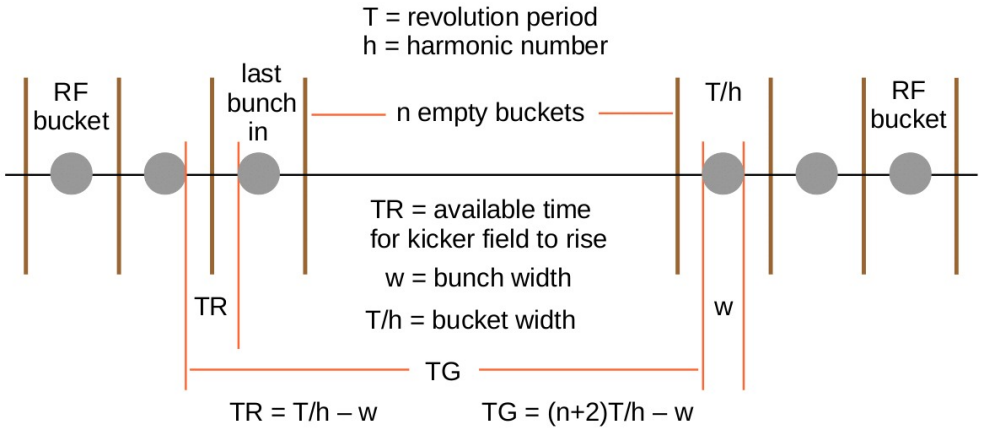

Figure 1: Timing for the injection of gold bunches into AGS RF buckets. Here T is the revolution period on the AGS injection porch and T/h is the width of the RF harmonic h bucket. The **time available** for the injection kicker magnetic field to rise is $T_R = T/h - w$, where w is the **width** of the bunch in the bucket. For injection of the last bunch, the kicker pulse must fit inside the **time gap** $T_G = (n+2)T/h - w$, where n is the number of empty buckets following the last bunch.

21 AGS injection kicker pulse

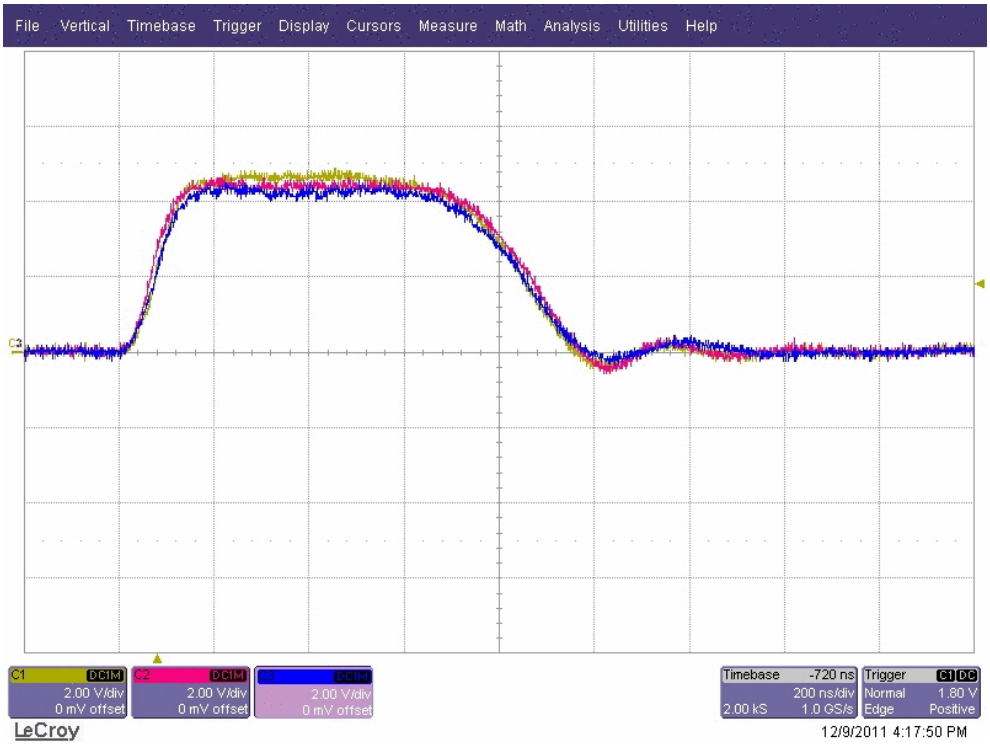

Figure 2: AGS injection kicker waveforms in the short pulse mode. The three traces are from the three modules of the kicker. They were taken by Yugang Tan on 9 Dec 2011. The time per division is 200 ns. The rise time of the pulse is approximately 100 ns. The width of the pulse is approximately 1000 ns.

22 Fill pattern and timing for 6 to 1 merge

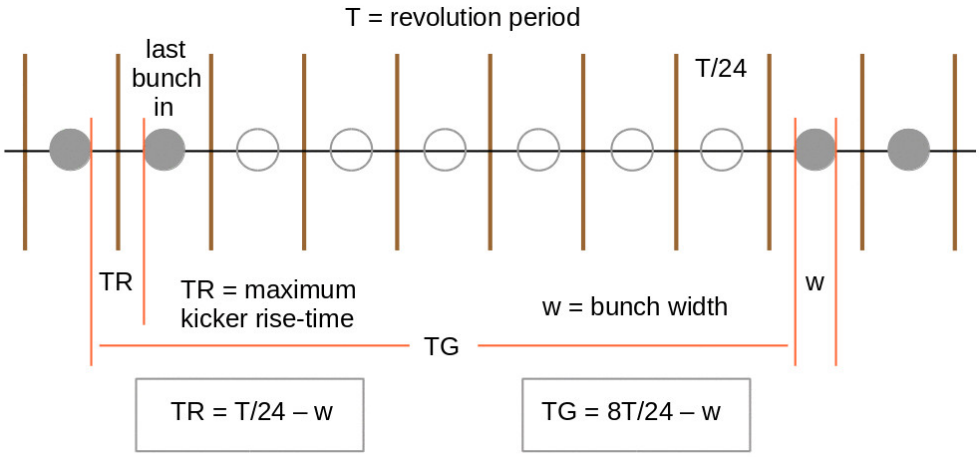

Figure 3: The fill pattern and merge described here were developed by K. Zeno and are documented in [1, 2]. As shown above, T is the revolution period on the AGS injection porch and $T/24$ is the width of the RF harmonic 24 bucket. The nominal revolution frequency at injection is 163.125 kHz, which gives $T/24 = 255$ ns. The time available for the kicker field to rise is $T/24 - w$, where w is the bunch width. The kicker rise time is 100 ns. This means that the bunch width must be less than $T/24 - 100 = 155$ ns. The fill pattern is 6 adjacent filled harmonic 24 buckets followed by 6 adjacent empty buckets, followed by another 6 adjacent filled buckets. This allows each group of 6 adjacent bunches to be merged into a single bunch. The **time gap available** for the kicker pulse is $8T/24 - w = 2040 - w$ ns, which is more than enough to accommodate the full width of the pulse. The 6 to 1 merge produces a merged bunch sitting in every other harmonic 4 bucket. Each bunch is then squeezed into a harmonic 12 bucket for subsequent acceleration as documented in [21, 22].

At extraction one has 2 bunches, each of which sits in its own harmonic 12 bucket and is separated from its neighbor by 5 empty buckets. The bucket widths ($T/12$) at extraction are listed in Sections 4 and 6 and range from 225 to 231 ns. The rise time and full width of the extraction kicker pulse are 292 and 672 ns respectively [23]. These are easily accommodated by the empty-bucket gaps between the bunches.

23 Fill pattern and timing for 4 to 1 merge

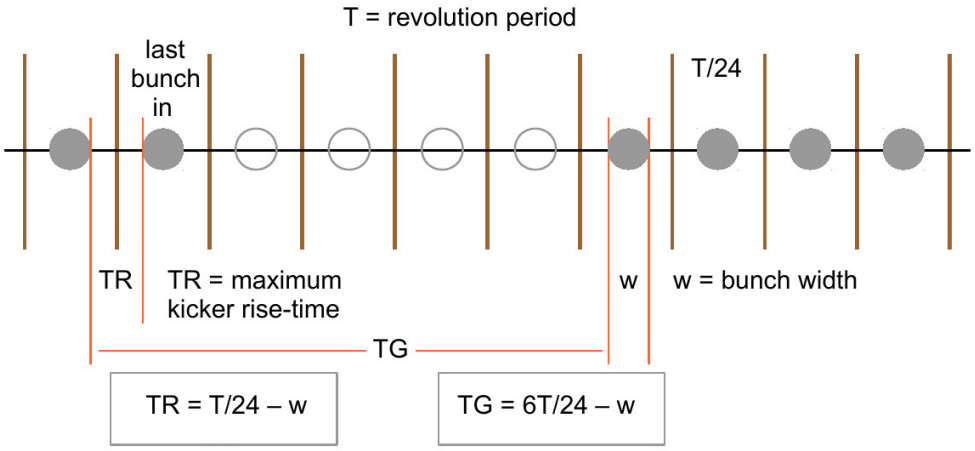

Figure 4: The fill pattern and merge described here were developed by K. Zeno this year [7]. The nominal revolution frequency at AGS injection is again 163.125 kHz, which gives $T/24 = 255$ ns. The time available for the kicker field to rise is $T/24 - w$, where w is the bunch width. The kicker rise time is 100 ns. The fill pattern is 4 adjacent filled harmonic 24 buckets followed by 4 adjacent empty buckets and so on until there are 3 groups of 4 adjacent filled buckets with each group separated from its neighbors by a gap of 4 adjacent empty buckets. This allows each group of 4 bunches to be merged into a single bunch. The **time gap available** for the kicker pulse is $6T/24 - w = 1530 - w$ ns, which is more than enough to accommodate the full width of the pulse. The 4 to 1 merge is accomplished by doing two 2 to 1 merges. The first is done on the injection porch. The second is done on a porch where the revolution frequency is high enough for the "KL" cavity to produce harmonic 6 buckets. One ends up with a merged bunch sitting in every other harmonic 6 bucket. Each bunch is then captured into a harmonic 12 bucket for subsequent acceleration. At extraction one has 3 bunches, each of which sits in its own harmonic 12 bucket and is separated from its neighbors by 3 empty buckets. The time available for the rise of the extraction kicker pulse is $4T/12 - w$, where w is the bunch width at extraction and $T/12$ ranges from 225 to 231 ns. The time gap available for the kicker pulse is $8T/12 - w$. These available times easily accommodate the rise time (292 ns) and full width (672 ns) of the extraction kicker pulse.

24 Fill pattern and timing for 3 to 1 merge

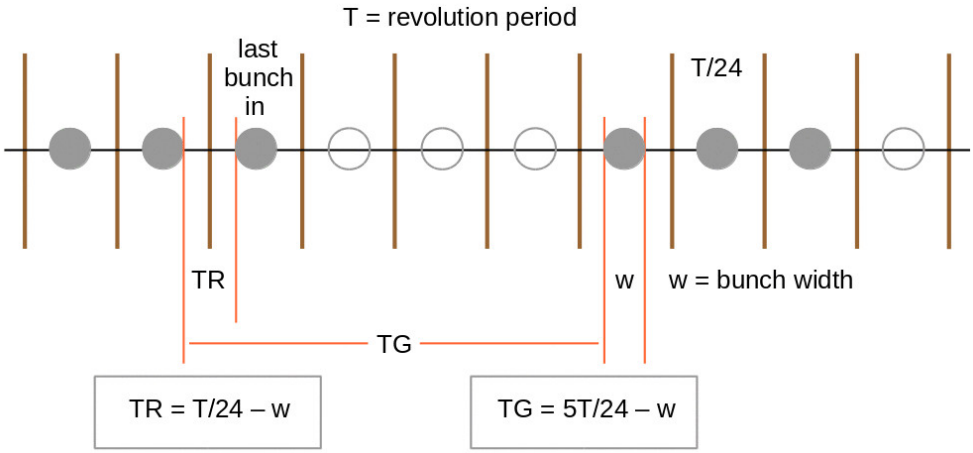

Figure 5: Here the nominal revolution frequency at AGS injection is again 163.125 kHz, which gives $T/24 = 255$ ns. The fill pattern is 3 adjacent filled harmonic 24 buckets followed by 3 adjacent empty buckets, followed by another 3 adjacent filled buckets and so on until there are 4 groups of three bunches. This allows each group of three bunches to be merged into a single bunch. The **time gap available** for the kicker pulse is $5T/24 - w$, which is enough to accommodate the width of the pulse. The 3 to 1 merge requires harmonics 24, 16, and 8 on the injection porch. Standard AGS RF cavities provide the harmonic 24 and 16 frequencies; the "KL" cavity is needed to provide harmonic 8. One ends up with a merged bunch sitting in every other harmonic 8 bucket. Each bunch is then captured into a harmonic 12 bucket for subsequent acceleration. All of this was set up by Iris Zhang and is documented in [24]. At extraction one has 4 bunches, each of which sits in its own harmonic 12 bucket and is separated from its neighbors by 2 empty buckets. The time available for the rise of the extraction kicker pulse is $3T/12 - w$, where w is the bunch width at extraction and $T/12$ ranges from 225 to 231 ns. The time gap available for the kicker pulse is $6T/12 - w$. These available times easily accommodate the rise time (292 ns) and full width (672 ns) of the extraction kicker pulse.

25 Fill pattern for an alternate 3 to 1 merge

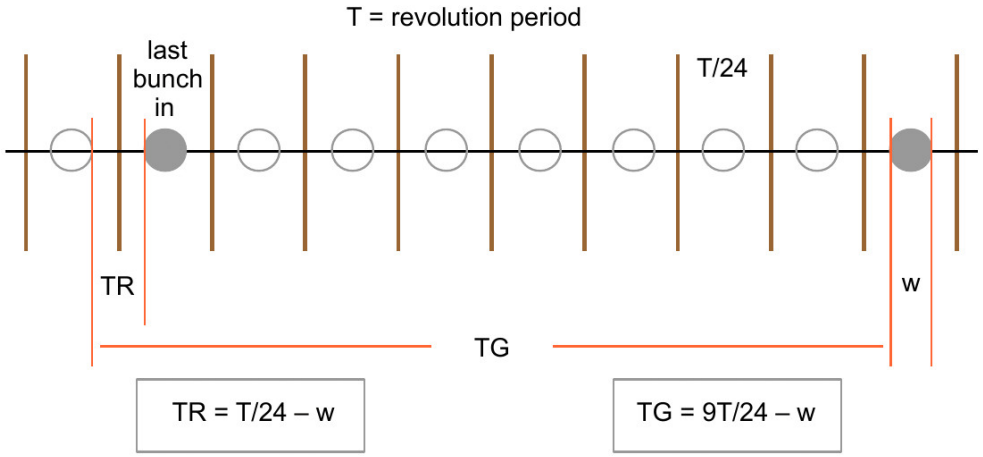

Figure 6: The fill pattern and merge described here were developed by K. Zeno [5]. The nominal revolution frequency at AGS injection is again 163.125 kHz, which gives $T/24 = 255$ ns. The fill pattern is a bunch in every other harmonic 24 bucket outside the gap of 7 empty buckets shown above. The **time gap available** for the kicker pulse is $9T/24 - w$, which is more than enough to accommodate the full width of the pulse. The fill pattern gives a total of 9 filled harmonic 24 buckets. These are captured into 9 adjacent harmonic 12 buckets and accelerated to a merging porch where a 3 to 1 merge produces a merged bunch sitting in three of four harmonic 4 buckets. If the harmonic 24 buckets were populated so that a fourth merged bunch could occupy the remaining harmonic 4 bucket, then the gap for the injection kicker would be reduced to just $4T/24 - w$ which is too small. The merge requires harmonics 12, 8, and 4. The corresponding nominal RF frequencies are 2.349, 1.566, and 0.783 MHz, which are the same as those used in the 6 to 1 merge setup. Each merged bunch is squeezed into a harmonic 12 bucket for subsequent acceleration. At extraction one has 3 bunches, each of which sits in its own harmonic 12 bucket and is separated from its neighbors by 2 or 5 empty buckets. This gives ample room for both the rise time and full width of the extraction kicker pulse.

26 Fill pattern and timing for 2 to 1 merge

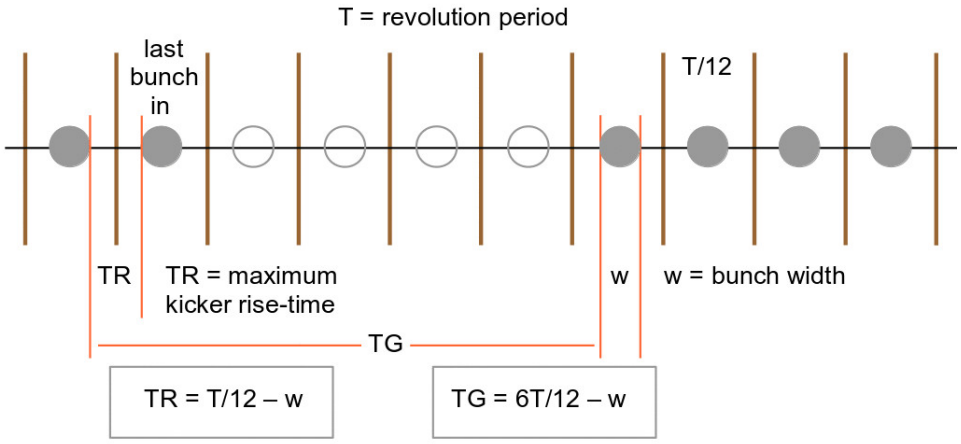

Figure 7: The fill pattern and merge described here are for the case in which Au31+ ions are provided by Tandem. These were developed by K. Zeno and are documented in [5]. The harmonic number at AGS injection is 12 and the nominal revolution frequency is 158.696 kHz. This gives $T/12 = 525$ ns. The time available for the injection kicker field to rise is $T/12 - w$, where w is the bunch width. The kicker rise time is 100 ns. The fill pattern is 8 adjacent filled harmonic 12 buckets followed by 4 adjacent empty buckets. The **time gap available** for the kicker pulse is $6T/12 - w$, which is more than enough to accommodate the full width of the pulse. The bunches are accelerated to a merging porch where the revolution frequency is high enough for the "KL" cavity to produce harmonic 6 buckets. A single 2 to 1 merge on the porch produces 4 bunches sitting in 4 adjacent harmonic 6 buckets. Each bunch is then captured into its own harmonic 12 bucket for subsequent acceleration. At extraction one has a bunch sitting in every other harmonic 12 bucket outside a gap of 5 empty buckets. The time available for the rise of the extraction kicker pulse is $2T/12 - w$, where w is the bunch width at extraction and $T/12$ ranges from 225 to 231 ns. The time gap available for the kicker pulse is at least $8T/12 - w$. These available times easily accommodate the rise time (292 ns) and full width (672 ns) of the extraction kicker pulse.

27 Fill pattern for an alternate 2 to 1 merge

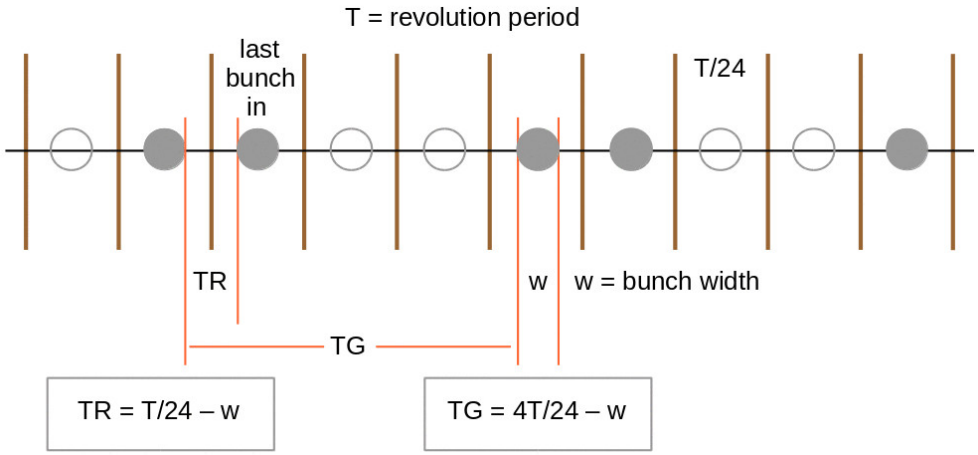

Figure 8: Here, as before, T is the revolution period on the AGS injection porch and $T/24$ is the width of the RF harmonic 24 bucket. The nominal revolution frequency at injection is 163.125 kHz. For the setup with Au31+ ions from Tandem, the revolution frequency is 158.696 kHz. The time available for the kicker field to rise is $T/24 - w$, where w is the bunch width. The kicker rise time is 100 ns. The fill pattern in this case is 2 adjacent filled harmonic 24 buckets followed by 2 adjacent empty buckets and so on until there are up to 6 groups of 2 bunches. This allows each group of 2 bunches to be merged into a single bunch. For the case in which there are 6 groups, the **time gap available** for the kicker pulse is $4T/24 - w$ which is not quite enough to accommodate the full width of the pulse. If there are less than 6 groups then there is ample room for the pulse. At extraction one then has at most 5 bunches, each of which sits in its own harmonic 12 bucket and is separated from its neighbors by at least one empty bucket. The time available for the rise of the extraction kicker pulse is $2T/12 - w$, where w is the bunch width at extraction and $T/12$ ranges from 225 to 231 ns. The time gap available for the kicker pulse is at least $6T/12 - w$. These available times easily accommodate the rise time (292 ns) and full width (672 ns) of the extraction kicker pulse.

28 Temperature rise in the BTA stripper foils assuming no cooling

Following is a back-of-the-envelope calculation of the temperature rise in the aluminum and carbon foils assuming no cooling by heat flow or radiation.

The energy deposited as N Au77+ ions travel a small distance d in a foil is

$$E = -N \frac{dE}{dx} \rho d \tag{17}$$

where ρ is the density of the foil material and

$$-\frac{dE}{dx} = -Q^2 \frac{dE_p}{dx}. \tag{18}$$

Here the ion charge

$$Q = 77 \tag{19}$$

and $-dE_p/dx$ is the rate at which a proton loses energy while traveling through the foil with the same velocity as the ion.

As shown in **Section 15** we have

$$-\frac{dE_p}{dx} = 5.589 \text{ MeV cm}^2/\text{g} \text{ (aluminum)} \tag{20}$$

$$-\frac{dE_p}{dx} = 6.468 \text{ MeV cm}^2/\text{g} \text{ (carbon)} \tag{21}$$

in the aluminum and carbon foils. Thus we have

$$-\frac{dE}{dx} = 33.1372 \text{ GeV cm}^2/\text{g} \text{ (aluminum)} \tag{22}$$

$$-\frac{dE}{dx} = 38.3488 \text{ GeV cm}^2/\text{g} \text{ (carbon)}. \tag{23}$$

If the ions are incident on foil surface area A then the energy is deposited in mass

$$M = \rho A d. \tag{24}$$

The resulting temperature increase (assuming no heat flow or radiation) is

$$\Delta T = \frac{E}{cM} = -\frac{N}{cA} \frac{dE}{dx} \tag{25}$$

where c is the heat capacity of the foil material. Note that the factor ρd cancels out when (17) is divided by (24). The heat capacities of aluminum and carbon, respectively, are [25]

$$c_1 = 0.897 \text{ J/(gK)}, \quad c_2 = 0.709 \text{ J/(gK)}. \tag{26}$$

Taking

$$N = 1.0 \times 10^9 \text{ ions} \tag{27}$$

and area

$$A = 1.0 \text{ cm}^2 \tag{28}$$

and using

$$1 \text{ eV} = 1.602\,176\,634 \times 10^{-19} \text{ Joules} \tag{29}$$

we obtain temperature increases

$$\Delta T_1 = 5.92 \text{ K}, \quad \Delta T_2 = 8.67 \text{ K} \tag{30}$$

in the aluminum and carbon foils, respectively. These numbers may be scaled to obtain the temperature increases for any N or A.

For the setup discussed in **Section 16**, we had up to 9.6×10^9 Au77+ ions circulating in AGS at extraction. This required nearly 20×10^9 Au31+ ions entering the BTA transfer line per AGS cycle. These were delivered at a rate of one bunch of 2.5×10^9 ions per Booster cycle, with 8 such bunches delivered per AGS cycle. The Booster cycle time was 267 ms. As each bunch passes through a foil, the temperature of the affected part of the foil increases (assuming no cooling) by 2.5 times the amounts given in (30). The temperature increase after 8 bunches have passed through the foil would be 20 times the increases given in (30). This amounts to

$$\Delta T_1 = 118 \text{ K}, \quad \Delta T_2 = 173 \text{ K} \tag{31}$$

in the aluminum and carbon foils, respectively.

These numbers show that if cooling is ignored, the aluminum foil will reach its melting point (933.47 degrees K) in just 6 AGS cycles. Carbon, on the other hand, has no melting point at atmospheric pressure (or below), but undergoes sublimation at approximately 3915 degrees K (as per Wikipedia). With no cooling, the carbon foil would reach this temperature in 21 AGS cycles.

29 Formulae for the rate of radiative cooling

We have the following numbers:

1. The emissivity of aluminum from 50 to 500 degrees C is

$$\epsilon_1 = 0.04 \text{ to } 0.06 \text{ (aluminum)}. \tag{32}$$

2. The emissivity of carbon (graphite) from 0 to 3600 degrees C is

$$\epsilon_2 = 0.70 \text{ to } 0.80 \text{ (carbon)}. \tag{33}$$

3. The Stefan-Boltzmann constant is

$$\sigma = 5.6704 \times 10^{-8}\,\mathrm{W\,m^{-2}\,K^{-4}}. \tag{34}$$

We use subscripts 1 and 2 to denote parameters of the aluminum and carbon foils respectively. The two foils face one another with the aluminum foil situated just upstream of the carbon foil. One side of each foil faces and exchanges radiation with its neighbor. The other side faces and exchanges radiation with the vacuum chamber. The rate at which energy is radiated from the side facing the vacuum chamber is

$$P_W = A\epsilon\sigma\left(T^4 - T_W^4\right) \tag{35}$$

where T is the foil temperature and T_W is the temperature of the vacuum chamber wall. A is the radiating area under consideration. Similarly, the rate at which energy is radiated from the side facing the neighboring foil is

$$P_N = A\epsilon\sigma\left(T^4 - T_N^4\right) \tag{36}$$

where T_N is the temperature of neighboring foil. The total rate at which energy is radiated from a foil is then

$$P = P_W + P_N. \tag{37}$$

For the aluminum and carbon foils we therefore have

$$P_1 = A\epsilon_1\sigma\left(T_1^4 - T_W^4\right) + A\epsilon_1\sigma\left(T_1^4 - T_2^4\right) \tag{38}$$

$$P_2 = A\epsilon_2\sigma\left(T_2^4 - T_W^4\right) + A\epsilon_2\sigma\left(T_2^4 - T_1^4\right). \tag{39}$$

These equations show that if

$$T_2 = T_1 \tag{40}$$

then the net radiation from each foil comes only from the side facing the vacuum chamber. Note also that if the foil and its neighbor are identical then

$$\epsilon_1 = \epsilon_2 = \epsilon \tag{41}$$

and the rightmost terms in (38) and (39) cancel when P_1 and P_2 are added together. This is true for any values of T_1 and T_2. One would then have

$$P_1 + P_2 = A\epsilon\sigma\left(T_1^4 - T_W^4\right) + A\epsilon\sigma\left(T_2^4 - T_W^4\right) \tag{42}$$

for the net power radiated from the two foils. If $T_1 = T_2 = T$ then (42) would give

$$P_1 + P_2 = 2A\epsilon\sigma\left(T^4 - T_W^4\right) \tag{43}$$

which is just the power radiated from the two sides of a single foil.

In the next section we use (38) and (39) to calculate the temperature change in the foils as they cool after each energy deposition.

30 Energy deposition followed by radiative cooling

We ignore here any conduction of heat in the foils. The foil area A under consideration then cools only by radiation. The area is adjusted to give results consistent with observation. We again use subscripts 1 and 2 to denote parameters of the aluminum and carbon foils respectively.

We assume that energy is deposited instantaneously as each Booster load of ions passes through the foils. As shown in **Section 28**, the corresponding instantaneous increases in temperature are

$$\Delta T_1 = -\frac{\mathcal{N}}{c_1 A}\frac{dE_1}{dx}, \quad \Delta T_2 = -\frac{\mathcal{N}}{c_2 A}\frac{dE_2}{dx} \tag{44}$$

where

$$-\frac{dE_1}{dx} = 33.1372 \text{ GeV cm}^2/\text{g}, \quad -\frac{dE_2}{dx} = 38.3488 \text{ GeV cm}^2/\text{g} \tag{45}$$

$$c_1 = 0.897 \text{ J/(gK)}, \quad c_2 = 0.709 \text{ J/(gK)} \tag{46}$$

and A is the area of energy deposition. $\mathcal{N}$ is the number of gold ions that pass through the foils per Booster load. This is given by

$$\mathcal{N} = N/L \tag{47}$$

where N is the total number of ions that pass through the foils per supercycle and L is the number of Booster loads delivered per supercycle.

For the 5.75 GeV per nucleon setup we have

$$12 \times 10^9 \leq N \leq 20 \times 10^9, \quad L = 8. \tag{48}$$

The periods of the Booster cycle and supercycle are 267 and 5600 ms respectively [7]. In each supercycle there are therefore 8 cooling periods of 267 ms followed by a longer 3464 ms cooling period.

After each energy deposition, the rates of temperature change due to radiative cooling are

$$\frac{dT_1}{dt} = \frac{-P_1}{c_1\rho_1 d_1 A}, \quad \frac{dT_2}{dt} = \frac{-P_2}{c_2\rho_2 d_2 A} \tag{49}$$

where, as shown in the previous section,

$$P_1 = A\epsilon_1\sigma\left(T_1^4 - T_W^4\right) + A\epsilon_1\sigma\left(T_1^4 - T_2^4\right) \tag{50}$$

$$P_2 = A\epsilon_2\sigma\left(T_2^4 - T_W^4\right) + A\epsilon_2\sigma\left(T_2^4 - T_1^4\right). \tag{51}$$

We therefore have two coupled first-order differential equations

$$\frac{dT_1}{dt} = -\frac{\epsilon_1\sigma}{c_1\rho_1 d_1}\left(2T_1^4 - T_2^4 - T_W^4\right) \tag{52}$$

$$\frac{dT_2}{dt} = -\frac{\epsilon_2\sigma}{c_2\rho_2 d_2}\left(2T_2^4 - T_1^4 - T_W^4\right) \tag{53}$$

which we write as

$$\frac{dT_1}{dt} = \mathcal{C}_1 T_W^4 - \mathcal{C}_1\left(2T_1^4 - T_2^4\right) \tag{54}$$

$$\frac{dT_2}{dt} = \mathcal{C}_2 T_W^4 - \mathcal{C}_2\left(2T_2^4 - T_1^4\right) \tag{55}$$

where

$$\mathcal{C}_1 = \frac{\epsilon_1\sigma}{c_1\rho_1 d_1}, \quad \mathcal{C}_2 = \frac{\epsilon_2\sigma}{c_2\rho_2 d_2} \tag{56}$$

and

$$c_1 = 0.897 \text{ J/(gK)}, \quad c_2 = 0.709 \text{ J/(gK)} \tag{57}$$

$$\rho_1 d_1 = 6.45 \text{ mg/cm}^2, \quad \rho_2 d_2 = 8.39 \text{ mg/cm}^2. \tag{58}$$

The emissivities of the foils are given in the previous section. Putting in numbers gives

$$\mathcal{C}_1 = 0.5880 \times 10^{-10}, \quad \mathcal{C}_2 = 6.6727 \times 10^{-10} \quad \text{s}^{-1}\,\text{K}^{-3}. \tag{59}$$

The coupled equations (54) and (55) are easily solved by fourth-order Runge-Kutta integration [26, 27]. We take

$$T_W = 300 \text{ K} \tag{60}$$

and assume that the foils are initially in thermal equilibrium with the vacuum chamber wall.

For the instantaneous temperature increases given by (44), we consider energy deposition areas

$$A = 0.50, \;\; 0.75, \;\; 1.00 \;\; \text{cm}^2. \tag{61}$$

Taking first

$$\underline{A = 0.50 \text{ cm}^2} \tag{62}$$

we obtain the aluminum foil temperature-vs-time traces shown in **Figures 9** and **10**. These show that after five or so supercycles, an equilibrium is reached in which the temperature repeatedly peaks at a temperature T_H and then cools to a temperature T_C just before the next set of Booster loads takes the temperature back to the peak. These temperatures are

$$T_H = 929, \;\; 868, \;\; 797 \;\; \text{K} \tag{63}$$

$$T_C = 772, \;\; 741, \;\; 702 \;\; \text{K} \tag{64}$$

for 20e9, 16e9, and 12e9 gold ions, respectively, incident on the aluminum foil per supercycle. The 929 K peak is very close to the 933.47 K melting point of aluminum. This is surely bad for the foil and is consistent with the observed damage. The 868 K peak is also close and presumably damaging. The differences between the peak and cooled temperatures are

$$T_H - T_C = 157, \;\; 127, \;\; 95 \;\; \text{K} \tag{65}$$

for the three intensities. These temperature changes occur over the 3731 ms cooling period after the 8th energy deposition in each supercycle.

Taking next

$$\underline{A = 0.75 \text{ cm}^2} \tag{66}$$

we obtain the aluminum foil temperature-vs-time traces shown in **Figure 11**. Here the temperatures T_H and T_C are

$$T_H = 822,\ 770,\ 711 \text{ K} \tag{67}$$

$$T_C = 716,\ 686,\ 647 \text{ K} \tag{68}$$

for 20e9, 16e9, and 12e9 gold ions, respectively, incident on the aluminum foil per supercycle. The peak temperatures here are some 100 K lower than those obtained with $A = 0.50$ cm^2. The temperature differences for the three intensities are

$$T_H - T_C = 106,\ 84,\ 64 \text{ K}. \tag{69}$$

Finally, taking

$$\underline{A = 1.00 \text{ cm}^2} \tag{70}$$

we obtain the aluminum foil temperature-vs-time traces shown in **Figure 12**. Here the temperatures T_H and T_C are

$$T_H = 756,\ 711,\ 658 \text{ K} \tag{71}$$

$$T_C = 677,\ 647,\ 610 \text{ K} \tag{72}$$

for 20e9, 16e9, and 12e9 gold ions, respectively, incident on the aluminum foil per supercycle. The peak temperatures here are significantly lower than those obtained with $A = 0.50$ cm^2 and are well away from the 933.47 K melting point. The temperature differences for the three intensities are

$$T_H - T_C = 79,\ 64,\ 48 \text{ K}. \tag{73}$$

Figures 13 and **14** show the temperature-vs-time traces obtained for the <u>carbon foil</u> assuming $A = 0.50$ cm^2. The temperatures T_H and T_C are

$$T_H = 838,\ 783,\ 719 \text{ K} \tag{74}$$

$$T_C = 669,\ 643,\ 610 \text{ K} \tag{75}$$

for 20e9, 16e9, and 12e9 gold ions, respectively, incident on the aluminum foil per supercycle. These temperatures are well below the 3915 K sublimation temperature of carbon.

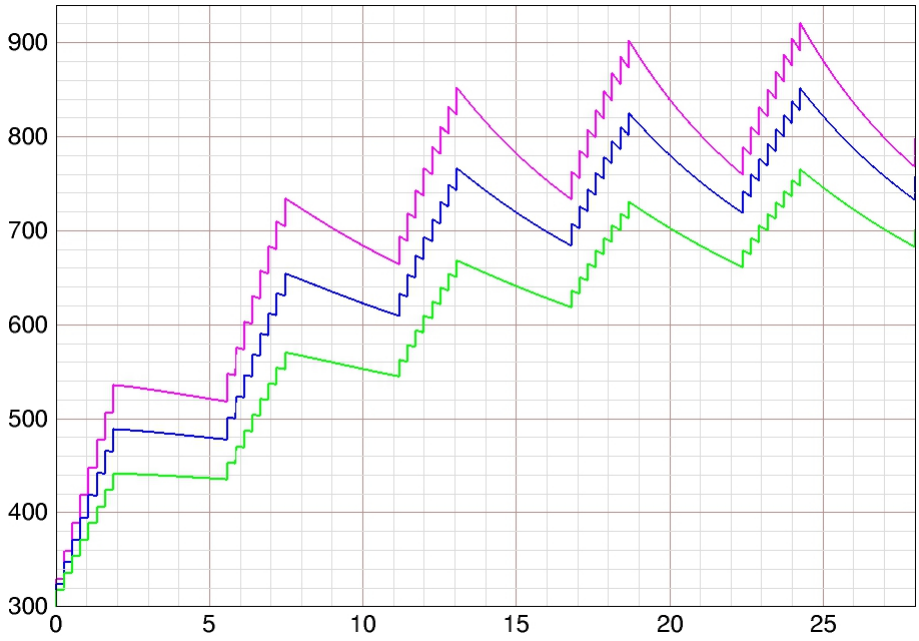

Figure 9: Aluminum foil temperature over 5 supercycles with $\underline{A = 0.50}$ cm^2. The horizontal axis gives the time in seconds. The vertical axis gives the temperature in degrees K. The melting point of aluminum is 933.47 K. The green (lower), blue (middle), and pink (upper) traces show the temperature for intensities of 12e9, 16e9, and 20e9 gold ions incident on the foil per supercycle. The Booster and supercycle periods are 267 and 5600 ms respectively.

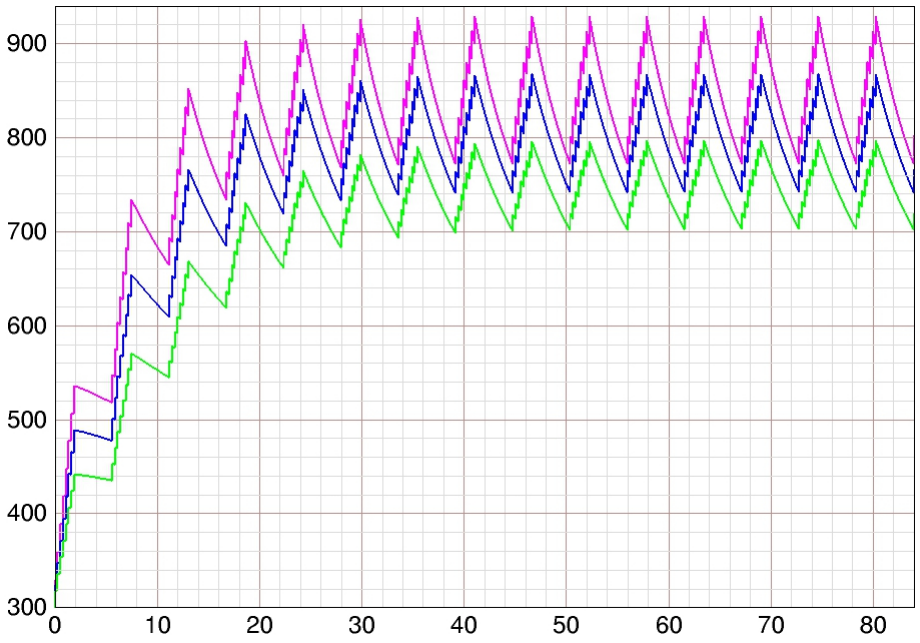

Figure 10: Aluminum foil temperature over 15 supercycles with $A = 0.50$ cm^2. The horizontal axis gives the time in seconds. The vertical axis gives the temperature in degrees K. The melting point of aluminum is 933.47 K. The green (lower), blue (middle), and pink (upper) traces show the temperature for intensities of 12e9, 16e9, and 20e9 gold ions incident on the foil per supercycle. In each trace an equilibrium is reached in which the temperature repeatedly peaks at a temperature T_H and cools to a temperature T_C. At the highest intensity (pink trace) these temperatures are 929 and 772 K respectively. Here T_H is very close to the aluminum melting point. At the middle intensity (blue trace) T_H and T_C are 868 and 741 K. At the lowest intensity (green trace) these temperatures are 797 and 702 K. The Booster and supercycle periods are 267 and 5600 ms respectively.

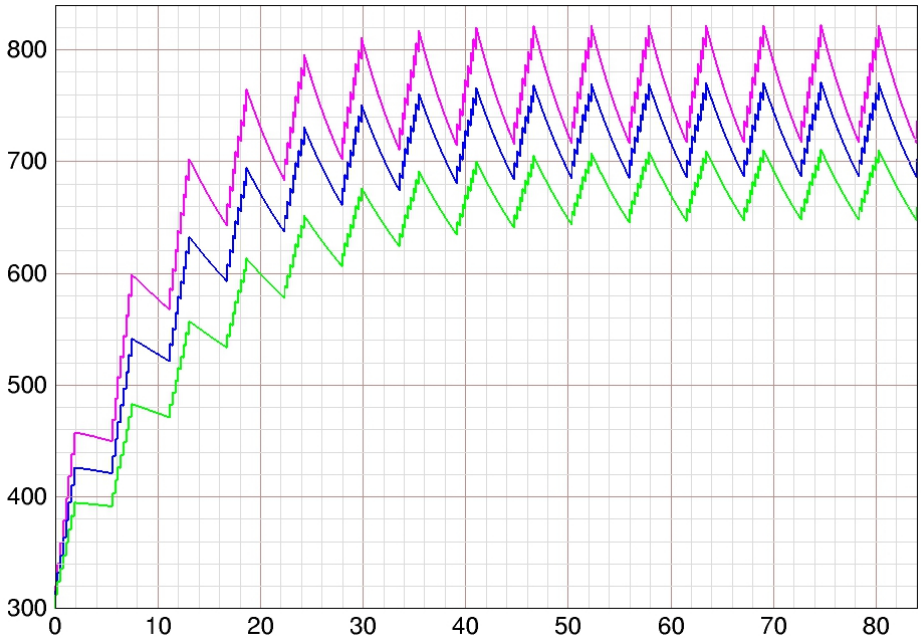

Figure 11: Aluminum foil temperature over 15 supercycles with $A = 0.75$ cm^2. The horizontal axis gives the time in seconds. The vertical axis gives the temperature in degrees K. The melting point of aluminum is 933.47 K. The green (lower), blue (middle), and pink (upper) traces show the temperature for intensities of 12e9, 16e9, and 20e9 gold ions incident on the foil per supercycle. In each trace an equilibrium is reached in which the temperature repeatedly peaks at temperature T_H and cools to temperature T_C. At the highest intensity (pink trace) these temperatures are 822 and 716 K respectively. At the middle intensity (blue trace) the temperatures are 770 and 686 K. At the lowest intensity (green trace) the temperatures are 711 and 647 K. The peak temperatures here are some 100 K lower than those obtained with $A = 0.50$ cm^2. The Booster and supercycle periods are 267 and 5600 ms respectively.

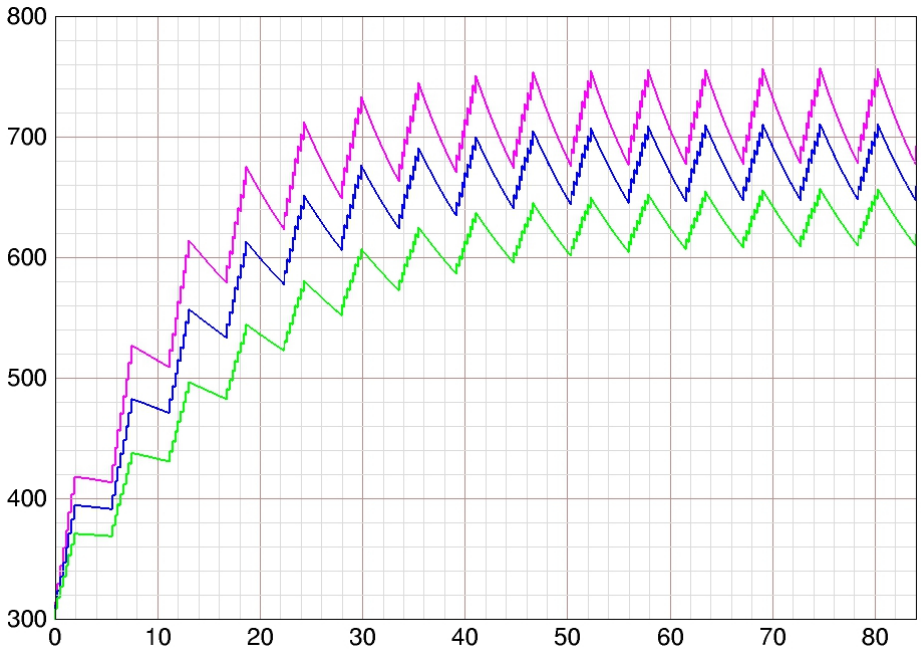

Figure 12: Aluminum foil temperature over 15 supercycles with $A = 1.00$ cm^2. The horizontal axis gives the time in seconds. The vertical axis gives the temperature in degrees K. The melting point of aluminum is 933.47 K. The green (lower), blue (middle), and pink (upper) traces show the temperature for intensities of 12e9, 16e9, and 20e9 gold ions incident on the foil per supercycle. In each trace an equilibrium is reached in which the temperature repeatedly peaks at temperature T_H and cools to temperature T_C. At the highest intensity (pink trace) these temperatures are 756 and 677 K respectively. At the middle intensity (blue trace) the temperatures are 711 and 647 K. At the lowest intensity (green trace) the temperatures are 658 and 610 K. The peak temperatures here are significantly lower than those obtained with $A = 0.75$ cm^2 and are well below the aluminum melting point. The Booster and supercycle periods are 267 and 5600 ms respectively.

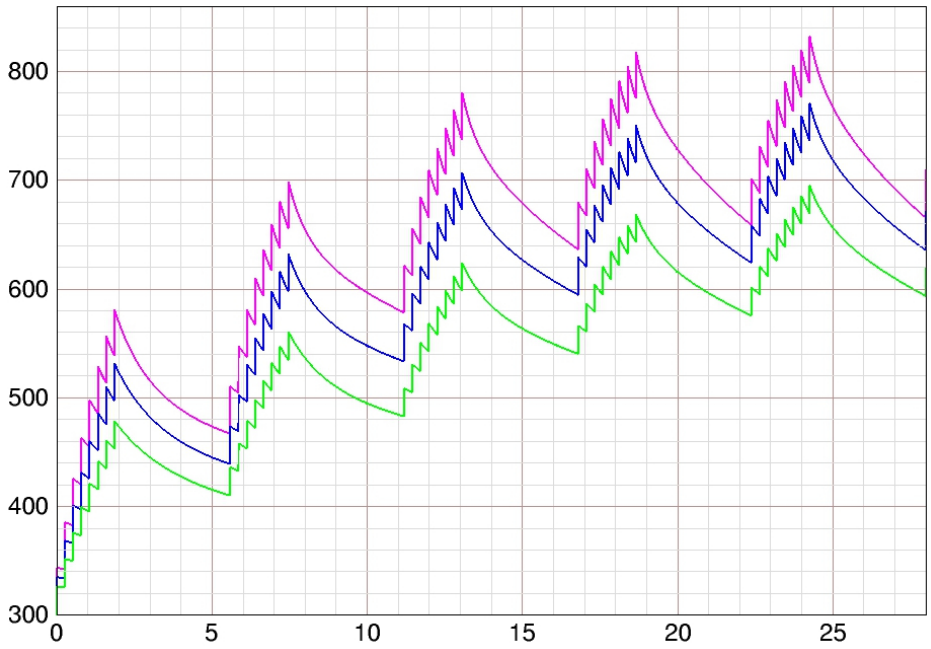

Figure 13: Carbon foil temperature over 5 supercycles with $A = 0.50$ cm^2. The horizontal axis gives the time in seconds. The vertical axis gives the temperature in degrees K. The sublimation temperature of carbon is 3915 K. The green (lower), blue (middle), and pink (upper) traces show the temperature for intensities of 12e9, 16e9, and 20e9 gold ions incident on the foil per supercycle. The Booster and supercycle periods are 267 and 5600 ms respectively.

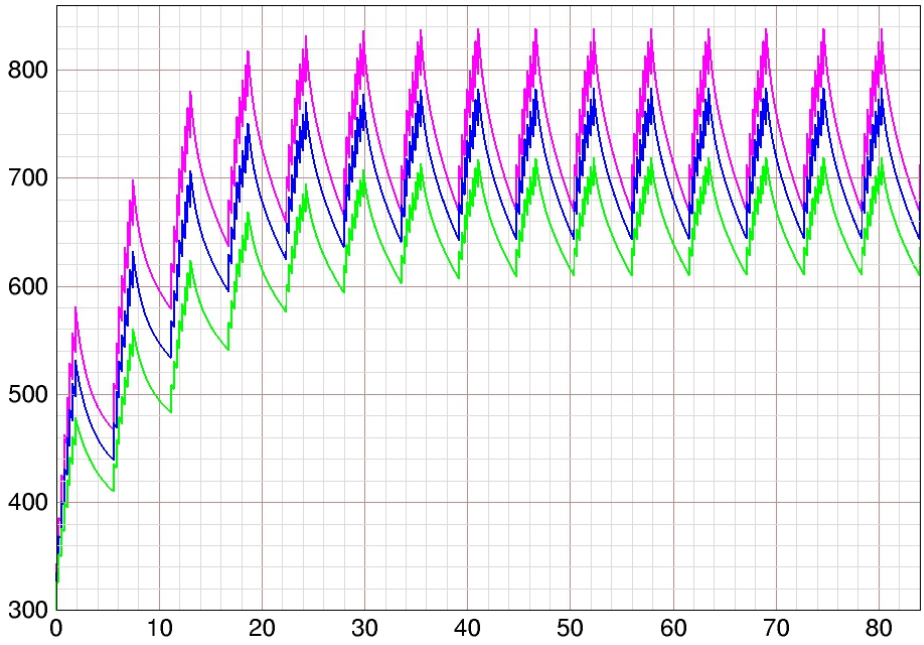

Figure 14: Carbon foil temperature over 15 supercycles with $A = 0.50$ cm^2. The horizontal axis gives the time in seconds. The vertical axis gives the temperature in degrees K. The sublimation temperature of carbon is 3915 K. The green (lower), blue (middle), and pink (upper) traces show the temperature for intensities of 12e9, 16e9, and 20e9 gold ions incident on the foil per supercycle. In each trace an equilibrium is reached in which the temperature repeatedly peaks at temperature T_H and cools to temperature T_C. At the highest intensity (pink trace) these temperatures are 838 and 669 K respectively. At the middle intensity (blue trace) the temperatures are 783 and 643 K. At the lowest intensity (green trace) the temperatures are 719 and 610 K. These temperatures are all well below the sublimation temperature of carbon. The Booster and supercycle periods are 267 and 5600 ms respectively.

31 Rates of gold ion energy loss in Copper

We consider gold ions traveling in copper at the energies 1, 2, 3, 4, 5 listed in **Sections 4** and **6**. The corresponding kinetic energies are

$$W/A = 2.9156,\ 3.6615,\ 4.8299,\ 6.3784,\ 8.8649\ \text{GeV/nucleon}. \tag{76}$$

The corresponding kinetic energies of protons having the same velocities as the ions are

$$W_p = 2.9379,\ 3.6896,\ 4.8669,\ 6.4273,\ 8.9328\ \text{GeV}. \tag{77}$$

The corresponding rates of energy loss of the protons in copper are [15]

$$-\frac{dE_p}{dx} = 1.409,\ 1.423,\ 1.450,\ 1.486,\ 1.534\ \text{MeV cm}^2/\text{g}. \tag{78}$$

The rates of energy loss of gold ions in copper are then given by [16]

$$-\frac{dE}{dx} = -Q^2\,\frac{dE_p}{dx} \tag{79}$$

where we take

$$Q = 79. \tag{80}$$

Putting in numbers one obtains

$$-\frac{dE}{dx} = 8.7936,\ 8.8809,\ 9.0495,\ 9.2741,\ 9.5737\ \text{GeV cm}^2/\text{g} \tag{81}$$

for gold ion energies 1, 2, 3, 4, 5 respectively.

32 Heating in the AGS beam dump

We use the results of the previous section to do a back-of-the-envelope calculation of beam-loss heating in the copper absorber of the AGS beam dump. The energy deposited as N Au79+ ions travel a small distance d in copper is

$$E = -N\frac{dE}{dx}\,\rho d \tag{82}$$

where $-dE/dx$ is given by (81) and ρ is the density of copper. If the ions are incident on surface area A then the energy is deposited in mass

$$M = \rho A d. \tag{83}$$

The resulting temperature increase (assuming no radiation or heat flow) is

$$\Delta T = \frac{E}{cM} = -\frac{N}{cA}\,\frac{dE}{dx} \tag{84}$$

where

$$c = 0.385 \text{ J/(gK)} \tag{85}$$

is the heat capacity of copper [25]. Note that the factor ρd cancels out when (82) is divided by (83).

Taking

$$N = 1.0 \times 10^9 \text{ ions} \tag{86}$$

and area

$$A = 1.0 \text{ cm}^2 \tag{87}$$

and using

$$1 \text{ eV} = 1.602\,176\,634 \times 10^{-19} \text{ Joules} \tag{88}$$

we obtain temperature increases

$$\Delta T = 3.6595,\ 3.6958,\ 3.7659,\ 3.8594,\ 3.9841 \text{ K} \tag{89}$$

for gold ion energies 1, 2, 3, 4, 5 respectively. These numbers may be scaled to obtain the temperature increases for any N or A.

For the case in which the plunging stripping foil is used to put gold beam into the upstream face of the dump, the area A appearing in (84) is estimated to be 0.25 cm^2 [18]. Taking

$$N = 9.6 \times 10^9 \text{ ions}, \quad A = 0.25 \text{ cm}^2 \tag{90}$$

in (84) then gives temperature increases that are (9.6/0.25) times those listed in (89). These are

$$\Delta T = 140.52,\ 141.92,\ 144.61,\ 148.20,\ 152.99 \text{ K} \tag{91}$$

for gold ion energies 1, 2, 3, 4, 5 respectively. Here we see that without any radiation or heat flow, the melting point of copper (1357.77 degrees K) would be reached in just a small number of AGS cycles.

33 Energy deposited in the dump per AGS cycle

Returning to (76) we have

$$W/A = 2.9156,\ 3.6615,\ 4.8299,\ 6.3784,\ 8.8649\ \text{GeV/nucleon} \tag{92}$$

for the kinetic energies of single Au77+ ions circulating in AGS at energies 1, 2, 3, 4, 5 listed in **Sections 4** and **6**. Multiplying by the number of nucleons ($A = 197$) and converting to Joules we have

$$W = 92.025,\ 115.57,\ 152.45,\ 201.32,\ 279.80\ \text{nJ}. \tag{93}$$

If N gold ions are put into the dump per AGS cycle then the total energy deposited is NW. For

$$N = 6.0 \times 10^9 \tag{94}$$

we have

$$NW = 552.15,\ 693.40,\ 914.67,\ 1207.9,\ 1678.8\ \text{J} \tag{95}$$

and for supercycle period

$$\mathcal{T} = 3.6\ \text{s} \tag{96}$$

we have power

$$NW/\mathcal{T} = 153.38,\ 192.61,\ 254.08,\ 335.53,\ 466.33\ \text{W}. \tag{97}$$

These are the rates at which heat must by removed from the dump copper. If N is increased to 9.6e9, these numbers increase by a factor of 1.6.

34 Rates of gold ion energy loss in Tungsten

We consider gold ions traveling in tungsten at the energies 1, 2, 3, 4, 5 listed in **Sections 4** and **6**. The corresponding kinetic energies are

$$W/A = 2.9156,\ 3.6615,\ 4.8299,\ 6.3784,\ 8.8649\ \text{GeV/nucleon}. \tag{98}$$

The corresponding kinetic energies of protons having the same velocities as the ions are

$$W_p = 2.9379,\ 3.6896,\ 4.8669,\ 6.4273,\ 8.9328\ \text{GeV}. \tag{99}$$

The corresponding rates of energy loss of the protons in tungsten are [15]

$$-\frac{dE_p}{dx} = 1.152,\ 1.168,\ 1.196,\ 1.231,\ 1.278\ \text{MeV cm}^2/\text{g}. \tag{100}$$

The rates of energy loss of gold ions in tungsten are then given by [16]

$$-\frac{dE}{dx} = -Q^2\,\frac{dE_p}{dx} \tag{101}$$

where we take

$$Q = 79. \tag{102}$$

Putting in numbers one obtains

$$-\frac{dE}{dx} = 7.1896,\ 7.2895,\ 7.4642,\ 7.6827,\ 7.9760\ \text{GeV cm}^2/\text{g} \tag{103}$$

for gold ion energies 1, 2, 3, 4, 5 respectively.

35 Heating in the AGS PSF

We use the results of the previous section to do a back-of-the-envelope calculation of beam-loss heating in the tungsten foil of the AGS plunging stripping foil (PSF).

The energy deposited as N Au79+ ions travel a small distance d in the tungsten foil is

$$E = -N\frac{dE}{dx}\,\rho d \tag{104}$$

where $-dE/dx$ is given by (103) and ρ is the density of tungsten. If the ions are incident on surface area A then the energy is deposited in mass

$$M = \rho A d. \tag{105}$$

The resulting temperature increase (assuming no radiation or heat flow) is

$$\Delta T = \frac{E}{cM} = -\frac{N}{cA}\,\frac{dE}{dx} \tag{106}$$

where

$$c = 0.134\ \text{J/(gK)} \tag{107}$$

is the heat capacity of tungsten [25]. Note that the factor ρd cancels out when (104) is divided by (105).

Taking

$$N = 1.0 \times 10^9 \text{ ions} \tag{108}$$

and area

$$A = 1.0 \text{ cm}^2 \tag{109}$$

and using

$$1 \text{ eV} = 1.602\,176\,634 \times 10^{-19} \text{ Joules} \tag{110}$$

we obtain temperature increases

$$\Delta T = 8.5963,\ 8.7157,\ 8.9246,\ 9.1859,\ 9.5365 \text{ K} \tag{111}$$

for gold ion energies 1, 2, 3, 4, 5 respectively. These numbers may be scaled to obtain the temperature increases for any N or A.

Taking

$$N = 9.6 \times 10^9 \text{ ions}, \quad A = 0.030 \text{ cm}^2 \tag{112}$$

gives temperature increases

$$\Delta T = 2750.8,\ 2789.0,\ 2855.9,\ 2939.5,\ 3051.7 \text{ K} \tag{113}$$

for gold ion energies 1, 2, 3, 4, 5 respectively. Here we see that without any radiation or heat flow, the melting point of tungsten (3695 K) would be reached in just two AGS cycles.

36 Heating and radiative cooling in the PSF

We ignore here any conduction of heat in the foil. The foil area A under consideration then cools only by radiation. The area is adjusted to give results consistent with observation. The emissivity of tungsten at 3600 K is

$$\epsilon = 0.35. \tag{114}$$

The analysis given in sections 16 and 17 of [18] shows that as the tungsten foil is plunged periodically (once per supercycle) into the circulating gold beam, an equilibrium is reached in which the temperature of the affected area repeatedly peaks at a temperature T_H and cools to a temperature T_C. That analysis was carried out with

$$\underline{N = 6.0 \times 10^9 \text{ ions}}, \quad A = 0.020 \text{ cm}^2, \quad \mathcal{T} = 3.6 \text{ s}, \quad \tau = 1.35 \text{ ms} \tag{115}$$

where $\mathcal{T}$ is the supercycle period and τ is the estimated energy deposition time. The resulting peak and cooled temperatures are

$$T_H = 3102.2,\ 3137.2,\ 3198.4,\ 3274.9,\ 3377.3\ \text{K} \tag{116}$$

$$T_C = 541.7,\ 541.8,\ 541.8,\ 541.9,\ 541.9\ \text{K} \tag{117}$$

for gold ion energies 1, 2, 3, 4, 5 respectively. These temperatures are well below the melting point of tungsten (3695 K).

Increasing N and A with

$$\underline{N = 8.0 \times 10^9 \text{ ions}}, \quad A = 0.023\ \text{cm}^2, \quad \mathcal{T} = 3.6\ \text{s}, \quad \tau = 1.35\ \text{ms} \tag{118}$$

gives temperatures

$$T_H = 3502.6,\ 3542.8,\ 3613.1,\ 3700.8,\ 3818.1\ \text{K} \tag{119}$$

$$T_C = 542.0,\ 542.0,\ 542.1,\ 542.1,\ 542.1\ \text{K} \tag{120}$$

for gold ion energies 1, 2, 3, 4, 5 respectively. Here we see that T_H goes above the melting point for energies 4 and 5. This is consistent with the evidence of melting found on the tungsten foil that was removed in October 2010 and examined under microscope by Peter Thieberger. His analysis of the observed foil erosion and melting is given in [28].

Increasing N and A further, and also increasing $\mathcal{T}$, we have

$$\underline{N = 9.6 \times 10^9 \text{ ions}}, \quad A = 0.028\ \text{cm}^2, \quad \mathcal{T} = 5.6\ \text{s}, \quad \tau = 1.35\ \text{ms} \tag{121}$$

which gives

$$T_H = 3394.9,\ 3434.7,\ 3504.2,\ 3590.9,\ 3707.0\ \text{K} \tag{122}$$

$$T_C = 473.1,\ 473.1,\ 473.1,\ 473.1,\ 473.2\ \text{K} \tag{123}$$

for gold ion energies 1, 2, 3, 4, 5 respectively. The peak temperature 3504.2 K obtained for energy 3 (5.75 GeV per nucleon) is consistent with the PSF "flash" observed in AGS at this energy and intensity. It is also consistent with the lack of any significant damage seen on the foil upon subsequent inspection. The temperature-vs-time trace obtained by Runge-Kutta integration for this energy and intensity is shown in **Figure 15**.

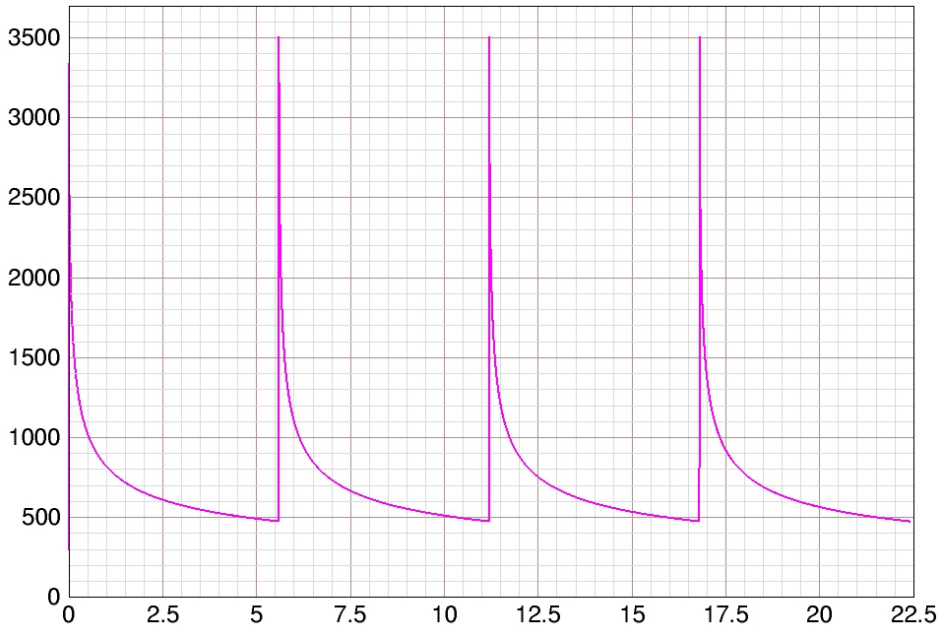

Figure 15: Tungsten foil temperature over 4 supercycles obtained by Runge-Kutta integration for energy 3 (5.75 GeV per nucleon) with $N = 9.6 \times 10^9$ gold ions per supercycle, energy deposition area $A = 0.028$ cm^2, supercycle period $\mathcal{T} = 5.6$ s, and energy deposition time $\tau = 1.35$ ms. The horizontal axis gives the time in seconds. The vertical axis gives the temperature in degrees K. The melting point of tungsten is 3695 K.

References

[1] K.L. Zeno, "Overview and analysis of the 2016 Gold Run in the Booster and AGS," C-A/AP/Note 571, September 2016.

[2] C.J. Gardner, "FY2016 Parameters for Gold Ions in Booster, AGS, and RHIC," C-A/AP/Note 574, October 2016.

[3] K.L. Zeno, Booster-AGS-EBIS elog, 11 February 2019.

[4] K.L. Zeno, "Run 16 Tandem gold performance in the injectors and possible improvement with AGS type 6:3:1 bunch merge in the Booster," C-A/AP/Note 576, October 2016.

[5] K.L. Zeno, "The 2019 Gold Run in the Injectors," C-A/AP/Note 627, November 2019.

[6] K.L. Zeno, Booster-AGS-EBIS elog, 22 November 2019.

[7] K.L. Zeno, "The 2020 Low Energy Gold Run in the Injectors," C-A/AP/Note 638, December 2020.

[8] C.J. Gardner, "Bucket and bunch parameters for clean injection of low energy gold ions into RHIC," C-A/AP/Note 607, July 2018.

[9] C.J. Gardner, "FY2014 Parameters for Gold Ions in Booster, AGS, and RHIC," C-A/AP/Note 525, July 2014.

[10] As given by Kevin Mernick.

[11] C.J. Gardner, "Notes on the setup of Ruthenium and Zirconium ions in Booster and AGS for RHIC Run 18," C-A/AP/Note 608, July 2018

[12] C.J. Gardner, "FY10 Parameters for the Injection, Acceleration, and Extraction of Gold Ions in Booster, AGS, and RHIC," C-A/AP/Note 397, August 2010.

[13] C.J. Gardner, et al, "Setup and Performance of the RHIC Injector Accelerators for the 2007 Run with Gold Ions", Proceedings of PAC07, pp. 1862–1864.

[14] P. Thieberger, et al, "Improved Gold Ion Stripping at 0.1 and 10 GeV/nucleon for the Relativistic Heavy Ion Collider", Phys. Rev. ST Accelerators and Beams **11**, 011001 (2008).

[15] M.J. Berger, J.S. Coursey, M.A. Zucker and J. Chang, "Stopping-Power and Range Tables for Electrons, Protons, and Helium Ions", www.nist.gov/physlab/data/star/index.cfm

[16] W.R. Leo, "Techniques for Nuclear and Particle Physics Experiments", Second Revised Edition, Springer-Verlag, 1994, pp. 24–28.

[17] C.J. Gardner, et al, "Operation of the RHIC Injector Chain with Ions from EBIS", Proceedings of IPAC2015, pp. 3804–3807.

[18] C.J. Gardner, L.A. Ahrens, and P. Thieberger, "Notes on Dumping Gold Beam in the AGS," C-A/AP/Note 396, August 2010.

[19] C.J. Gardner, H. Huang, and P.F. Ingrassia, "Temporary Procedure for increasing the intensity of Au77+ ions circulating in AGS at energy 5.75 GeV per nucleon," C-A-TPL 20-05, January 14, 2020.

[20] C.J. Gardner and H. Huang, "Temporary Procedure for increasing the intensity of Au77+ ions circulating in AGS at energy 3.85 or 5.75 GeV per nucleon," C-A-TPL 21-01, January 2021.

[21] C.J. Gardner, "Simulation of 6 to 3 to 1 merge and squeeze of Au77+ bunches in AGS," C-A/AP/Note 563, May 2016.

[22] C.J. Gardner, "Double and triple-harmonic RF buckets and their use for bunch squeezing in AGS," C-A/AP/Note 569, August 2016.

[23] Iris Zhang, Booster-AGS-EBIS elog, 20 March 2019. The rise time and full width of the AGS extraction kicker pulse are 292 ns and 672 ns respectively. The relative trigger times of the 4 kicker modules have been adjusted so that the length of the flat top portion of the resulting pulse is 119 ns. This is much longer than the flat top portion of the pulse from a single module and is needed to accommodate the longer bunch lengths at low energy.

[24] Iris Zhang, Booster-AGS-EBIS elog, 14 June and 10 July, 2019.

[25] Wikipedia, Heat capacities of the elements (data page).

[26] Neil Gershenfeld, "The Nature of Mathematical Modeling," Cambridge University Press, 1999, pp. 67–72.

[27] W.H. Press et al, "Numerical Recipes, FORTRAN Version," Cambridge University Press, 1989, pp. 550–560.

[28] P. Thieberger, "Plunging AGS stripper foil inspection and conclusions," unpublished presentation, October 2010.